Sánchez Tovar, R.; Lee, K.; García Antón, J.; Schmuki, P. (2013). Formation of anodic TiO2 nanotube or nanosponge morphology determined by the electrolyte hydrodynamic conditions. Electrochemistry Communications. 26:1-4. doi:10.1016/j.elecom.2012.09.041.

Formation of anodic TiO_2 nanotube or nanosponge morphology determined by the electrolyte hydrodynamic conditions

Rita Sánchez-Tovar[1,2], Kiyoung Lee[1], Jose García-Antón[2], Patrik Schmuki[1]*

[1]Department of Materials Science and Engineering, WW4-LKO, University of Erlangen-Nuremberg, Martensstrasse 7, D-91058 Erlangen, Germany

[2] Ingeniería Electroquímica y Corrosión, Departamento de Ingeniería Química y Nuclear, Universitat Politècnica de València, Camino de Vera s/n, 46022 Valencia, Spain

Abstract

The present work studies the effect of hydrodynamic conditions on the growth of anodic TiO_2 nanostructures on Ti in a glycerol/water/NH_4F electrolyte. Parameter screening for fluoride content, anodization voltage and rotation rate (Reynolds number) of a rotating anode showed that two distinctly different TiO_2 morphologies could be obtained: the classic ordered nanotubes or a nanoscale sponge layer. We present conditions for TiO_2 sponge formation and growth to several μm thickness, and show that in specific cases sponge layers can be superior to tube morphologies, as illustrated for photoelectrochemical water-splitting under standard AM 1.5 conditions.

Keywords: TiO_2, self-organization, porous structure, anodization.

* Corresponding author: Tel.: +49-9131-852-7575, Fax.: +49-9131-852-7582

E-mail: schmuki@ww.uni-erlangen.de

1. Introduction

Self-organized oxide layers formed by anodization of metals under a set of specific experimental conditions have over the past years attracted considerable interest in science and technology [1-3]. Particularly, ordered metal-oxide structures formed from highly functional oxides such as TiO_2 may find wide application in dye-sensitized solar cells [4-5], photocatalysis [6-10], biomedicine [11], and other related fields. While a number of different self-organized oxide morphologies can be anodically grown on Ti (for example nanochannels [12], fishbone structures [13], or loose nanotube bundles [14]), the most investigated structures over the past years were self-aligned TiO_2 nanotubes [2-3].

For growing these nanotube layers, dilute fluoride anion containing electrolytes are used [15]. Extensive work has been performed on optimizing anodization conditions and evaluate the influence of parameters such as pH, water content, fluoride content, or anodization voltage on the feasibility to form tubes and the influence on the resulting geometry [16-21]. The majority of these efforts used static electrolytes or electrolytes agitated under not well defined conditions such as magnetic stirring [21]. However, recently we showed, using a rotating electrode configuration, that hydrodynamic conditions can significantly affect the TiO_2 nanotube growth rate and the final tube geometry [22]. In the present work, we show that under specific anodization and hydrodynamic conditions (typically more drastic anodization conditions), a transition from a TiO_2 nanotube morphology to a nanosponge morphology occurs. We define the key parameters for sponge formation and explore potential use for this morphology.

2. Experimental

To perform anodization under defined hydrodynamic conditions, a 3-electrode electrochemical cell with a rotating electrode configuration was used. The anode was a Teflon coated titanium rod (12 mm diameter, 99.7% purity, Chempur, Germany) in a rotating electrode (AFMSRCE, Pine Research Instruments) set up. For all experiments, 1.13 cm^2 of the sample were exposed; for this in each run, the Ti rod front surface was abraded with 320 and 500 silicon carbide (SiC) papers. Then, it was polished with 9 μm polycrystalline diamond suspension and with a mixture composed by a colloidal silica polishing suspension and H_2O_2 (90:10 vol.%). After this, the sample was sonicated in ethanol for 2 min and dried in a N_2 stream. For anodization a Jaissle IMP 88-200 PC potentiostat was used, where the Ti rod served as working electrode, a platinum sheet as counter electrode and a platinum wire as a pseudo reference electrode. Different rotation speeds were used: 0, 228, 1075 and 1931 rpm corresponding to Reynolds numbers (Re) of 0, 65, 350, and 654. The Reynolds numbers (Re) were calculated as follows:

$$\mathrm{Re} = \frac{\omega r^2 \rho}{\mu} \quad (1)$$

where ω is the rotation speed expressed in $rad \cdot s^{-1}$, r is the radius of the working electrode in cm and ρ and μ are the density in $g \cdot cm^{-3}$ and dynamic viscosity in $g \cdot cm^{-1} \cdot s^{-1}$ of the solution, respectively [23].

After each test, a field-emission scanning electron microscope (Hitachi FE-SEM S4800) was used for morphological characterization of the obtained samples. X-ray diffraction analysis (XRD) was performed with a Philips X'pert MPD with a Panalytical X'celerator detector using graphite-monochromatized Cu Kα radiation.

The specimens were anodized at different potentials (from 5 V to 60 V) by increasing the potential from zero to the desired value at a rate of 200 $mV \cdot s^{-1}$, followed by keeping the end potential for a given time. The electrolyte for these experiments was a mixture of glycerol/water/ammonium fluoride at different concentrations: 0.27 M NH_4F in glycerol/water (60:40 vol. %), 0.135 M NH_4F in glycerol/water (60:40 vol. %), and 0.27 M NH_4F in glycerol/water (50:50 vol. %). Some experiments were performed at higher ammonium fluoride concentration (1 M) for the glycerol/water (60:40 vol. %) solution.

For photoelectrochemical water splitting measurements, the as-formed TiO_2 layers were annealed in a furnace at 450 °C in air for 1 h. The photoelectrochemical experiments were carried out under simulated sunlight condition AM 1.5 ($100 mW/cm^2$) in 1 M KOH solution. A three-electrode configuration was used, where TiO_2 layers were the working electrode (photoanode), a saturated Ag/AgCl (3 M KCl) the reference electrode, and a platinum foil the counter electrode. Photocurrent vs. voltage characteristics were recorded by scanning the potential from -0.840 V to +0.500 V with a scan rate of 1 mV/s using a Jaissle IMP 88 PC potentiostat. Photocurrent transients as a function of the applied potential were recorded by chopped light irradiation (60 s in the dark and 20 s in the light).

3. Results and discussion

Figure 1 illustrates the effect of the hydrodynamic conditions on the formation of anodic TiO_2 nanostructures. Figure 1a shows TiO_2 nanotubes grown in 0.27 M NH_4F containing glycerol/water (60:40 vol. %) electrolyte at 30 V - this well established morphology is obtained under static conditions, that is under 0 rpm of the rotating

electrode. If rotation of 228 rpm is used – keeping the rest of the anodization parameters constant - an entirely different morphology, a nanoporous "sponge", as shown in figure 1b is obtained. The layer, in this case, is ≈3.25 μm thick and consists of a connected TiO_2 structure with typical feature size in the range of 50 to 100 nm and pore openings of ≈30 nm.

Figure 1c and d show the electrochemical characteristics for Ti rod anodization at different rotation rates. Figure 1c shows the current-voltage behavior during the sweep from the 0 to 30 V with a sweep rate of 200 mV s^{-1} and figure 1d shows the subsequent current–time behavior recorded at 30 V during 3 h.

During the potential sweep, the current density shows a typical behavior observed for tube formation with a current maximum-minimum behavior [21]. Working under rotation smoothens the current-voltage behavior. Once the current sweep is finalized reaching the maximum of current density value, it gradually decreases and eventually reaches to a steady state level which represents a final state of an oxide formation/dissolution equilibrium [21].

Accordingly, larger steady state currents, that are observed for higher rotation rates, correspond to an accelerated oxide growth/dissolution equilibrium – in other words, sponge layer formation occurs at higher reaction rates.

Figure 1e shows the TiO_2 layer thickness as a dependence of the rotation speed for two different fluoride concentrations for an anodization time of 3 h. The inset gives the evolution of thickness of the layer at a fixed rotation rate over time. Please note that under these conditions only for a static electrolyte (0 rpm) a nanotubular (NT) morphology is obtained – all agitated conditions lead to a sponge morphology. From Figure 1e, it is clear that the sponge layer thickness increases with rotation speed and

time but tends to reach a limiting value. This final thickness depends mainly on the fluoride concentration. In this case a higher fluoride concentration leads to a higher steady state thickness, due to a higher turnover rate in the formation/dissolution equilibrium – this also corresponds to the observation of significantly higher steady state currents for higher fluoride concentrations (not shown).

Figure 1f shows the X-ray diffraction patterns (XRD) of the as-formed TiO_2 nanotubes and as-formed nanosponge structures. Clearly not only the as-formed tubes but also the sponge structure is amorphous.

Systematic investigation of additional parameters such as water content and potential allowed us to compile Figure 2 – where regions of existence of the different morphologies are shown as a function of the most influential parameters (rotation speed (Re), NH_4F concentration and applied voltage). Please note that also a transition region is included in Figure 2 where a mix between tubular and sponge morphology was observed. Moreover, particularly for low fluoride contents, neither a tube nor a sponge morphology could be observed but simply the presence of a compact oxide layer. From Figure 2, it is clear that NH_4F concentration, voltage and agitation influence the morphology - agitation always facilitates the transition to sponge formation.

The obtained sponge morphology, that is a connected nanoporous network, is potentially interesting for various typical TiO_2 applications. One of the most investigated applications of TiO_2 is its use for photocatalytic water splitting. To investigate this aspect we converted the as-formed amorphous structure to anatase (Figure 1f) by a thermal treatment at 450 ^{o}C in air. Preliminary experiments showed the sponge structure to be most effective at layer thickness between 500 nm to 1 μm. Therefore, we formed 500 nm to 1 μm thick sponge layers according to Figure 2, by the

anodization under static conditions, increasing the potential until 60 V at 200 $mV \cdot s^{-1}$ and holding at 60 V for 0 and 15 min in in 0.27 M NH_4F containing glycerol/water (60:40 vol. %) electrolytes. For comparison, nanotube layers were prepared by anodization at 30 V and 200 $mV \cdot s^{-1}$ for 0 and 1 h in the same electrolyte.

Both morphologies were annealed to anatase and photoelectrochemical water-splitting experiments were carried out by sweeping the potential in a 1 M KOH solution while periodically exposing the surface to AM 1.5 illumination (Figure 3). The resulting photocurrent transients show that for the same length the sponge layers lead to a higher photocurrent density. In fact, the smaller the layer thickness, the better is the relative performance of the sponge compare with the tubes. This may be ascribed to the higher surface area that is typically observed for example for nanoparticle assemblies (resembling the sponge). Nevertheless, with a higher thickness, the better electron transport properties in tubes become increasingly important [24]. For the investigated 0.5 μm layers, however, an almost twice increased photocurrent performance was obtained for the sponge morphology and this over the entire voltage range. While for tubes significantly higher photocurrent have been reported [25] the present results illustrate that for short aspect ratio the non-tubular morphologies can be superior.

In summary, the present work demonstrates that control of hydrodynamic conditions can be used to induce a morphology change when growing anodic oxide structures. A higher agitation rate can lead to the formation of a nanoporous sponge morphology which provides new features for various TiO_2 applications.

Acknowledgments

The authors would like to express their gratitude to the Spanish Ministry of

Science and Innovation FPU grant given to Rita Sánchez Tovar as well as DFG, and the DFG Cluster of Excellence at the University of Erlangen-Nuremberg [Engineering of Advanced Materials (EAM)] for financial support. We also like to thank the reviewer for valuable input.

References

[1] H. Masuda, K. Fukuda, Science 268 (1995) 1466.

[2] P. Roy, S. Berger, P. Schmuki, Angew. Chem. Int. Ed. 50 (2011) 2904.

[3] K.R. Hebert, S.P. Albu, I. Paramasivam, P. Schmuki, Nature Materials 11 (2012) 162.

[4] B. O´Regan, M. Grätzel, Nature 353 (1991) 737.

[5] P. Roy, D. Kim, K. Lee, E. Spiecker, P. Schmuki, Nanoscale 2 (2010) 45.

[6] A. Fujishima, T. N. Rao, D.A. Tryk, J. Photochem. Photobio. C: Photochem. Rev. 1 (2000) 1.

[7] A. Fujishima, X. Zhang, D.A. Tryk, Surf. Sci. Rep. 63 (2008) 515.

[8] K. Maeda, K. Domen, J. Phys. Chem. Lett. 1 (2010) 2655.

[9] J.H. Park, S. Kim, A.J. Bard, A. Nano Lett. 6 (2006) 24.

[10] J.M. Macak, M. Zlamal, J. Krysa, P. Schmuki, Small 3 (2007) 300.

[11] J. Park, S. Bauer, K. Von Der Mark, P. Schmuki, Nano Lett. 7 (2007) 1686.

[12] K. Lee, D. Kim, P. Schmuki, Chem. Commun. 47 (2011) 5789.

[13] K. Lee, D. Kim, P. Roy, I. Paramasivam, B.I. Birajdar, E. Spiecker, P, Schmuki, J. Am. Chem. Soc. 132 (2010) 1478.

[14] R. Hahn, J.M. Macak, P. Schmuki, Electrochem. Commun. 9 (2007) 947.

[15] V. Zwilling, E. Darque-Ceretti, A. Boutry-Forveille, D. David, M.Y. Perrin, M. Aucouturier, Surf. Interface Anal. 27 (1999), 629.

[16] J.M. Macak, H. Tsuchiya, P. Schmuki, Angew. Chem. Int. Ed. 44 (2005) 2100.

[17] W. Wei, S. Berger, C. Hauser, K. Meyer, M. Yang, P. Schmuki, Electrochem. Commun. 12 (2010) 1184.

[18] K.S. Raja, T. Gandhi, M. Misra, Electrochem. Commun. 9 (2007) 1069.

[19] S. Bauer, S. Kleber, P. Schmuki, Electrochem. Commun. 8 (2006) 1321.

[20] S.P. Albu, P. Roy, S. Virtanen, P. Schmuki, Isr. J. Chem. 50 (2010) 453.

[21] J.M. Macak, H. Hildebrand, U. Marten-Jahns, P. Schmuki, J. Electroanal. Chem. 621 (2008) 254.

[22] R. Sánchez-Tovar, I. Paramasivam, K. Lee, P. Schmuki, J. Mater. Chem. 22 (2012) 12792.

[23] N.-S. Cheng, Ind. Eng. Chem. Res. 47 (2008) 3285.

[24] R.P. Lynch, A. Ghicov, P, Schmuki J. Electrochem. Soc. 157 (2010) G76.

[25] I. Paramasivam, H. Jha , N. Liu , P. Schmuki, Small (2012) DOI: 10.1002/smll.201200564.

Figure captions

Figure 1. Cross sectional SEM images of (a) TiO_2 nanotubes formed in 0.27 M NH_4F containing glycerol/water (60:40 vol %) at 30 V for 3 h at 0 rpm and (b) TiO_2 nanosponge formed in 0.27 M NH_4F containing glycerol/water (60:40 vol %) at 30 V for 3 h at 228 rpm. (c) Current density versus potential during potential sweeping and (d) current density versus time during anodization in 0.27 M NH_4F containing glycerol/water (60:40 vol %) at 30 V for 3 h. (e) Layer thickness versus Re as function of NH_4F concentration. Inset shows layer thickness as function of anodization time. (f) XRD patterns for TiO_2 layers before and after annealing treatment at 450 ºC for 1 h.

Figure 2. Regions of existence of TiO_2 nanotubes and sponges.

Figure 3. Photocurrent transient vs. potential curves a for 1 μm and 0.5 μm nanosponges and nanotubes under AM 1.5 condition.

Figure 1.

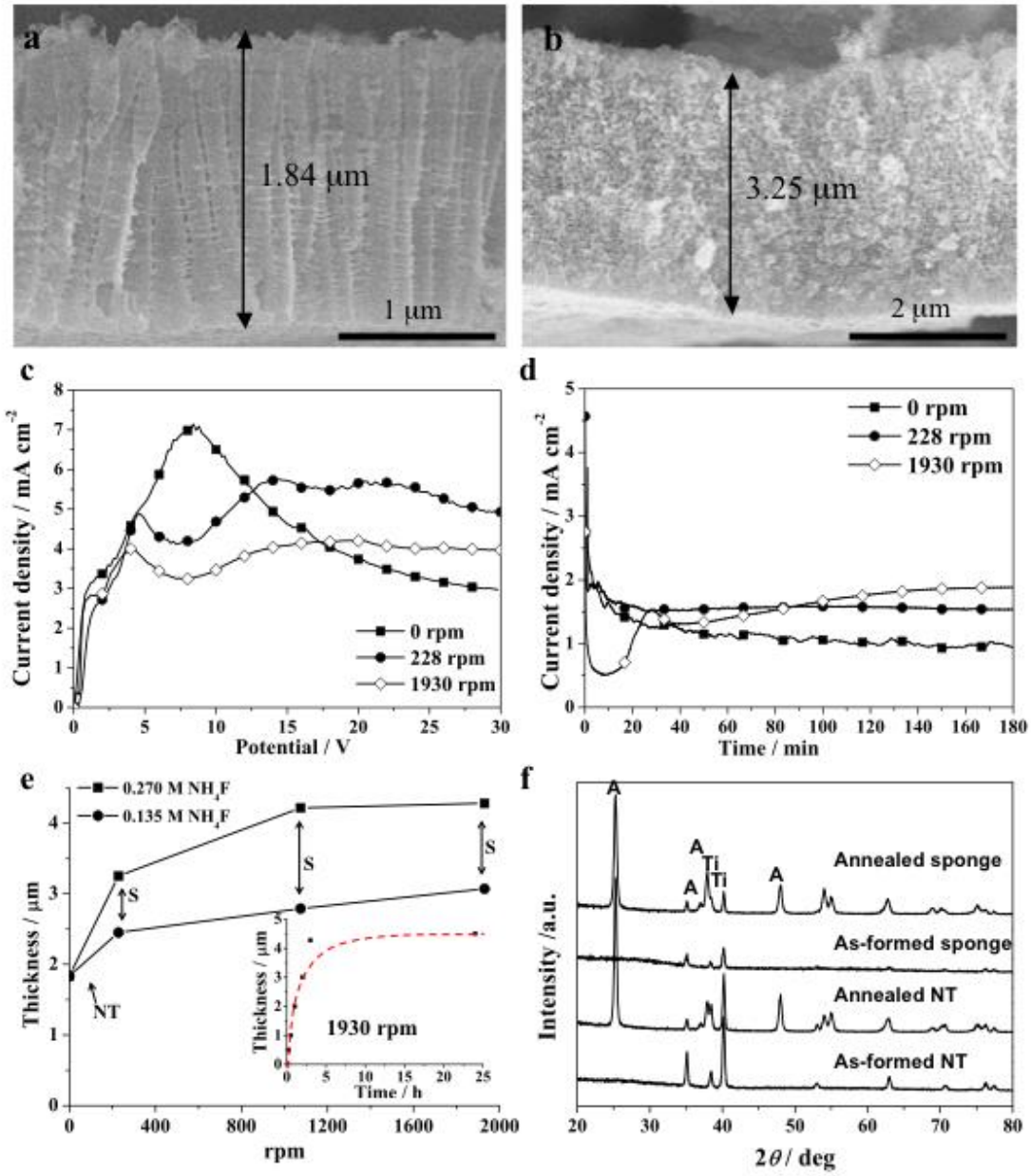
a
1.84 μm
1 μm
b
3.25 μm
2 μm
c
Current density / mA cm-2
Potential / V
0 rpm
228 rpm
1930 rpm
d
Current density / mA cm-2
Time / min
0 rpm
228 rpm
1930 rpm
e
0.270 M NH4F
0.135 M NH4F
S
S
S
NT
Thickness / μm
rpm
Thickness / μm
Time / h
1930 rpm
f
A
A
Ti
Ti
A
A
Annealed sponge
As-formed sponge
Annealed NT
As-formed NT
Intensity /a.u.
2θ / deg

Figure 2.

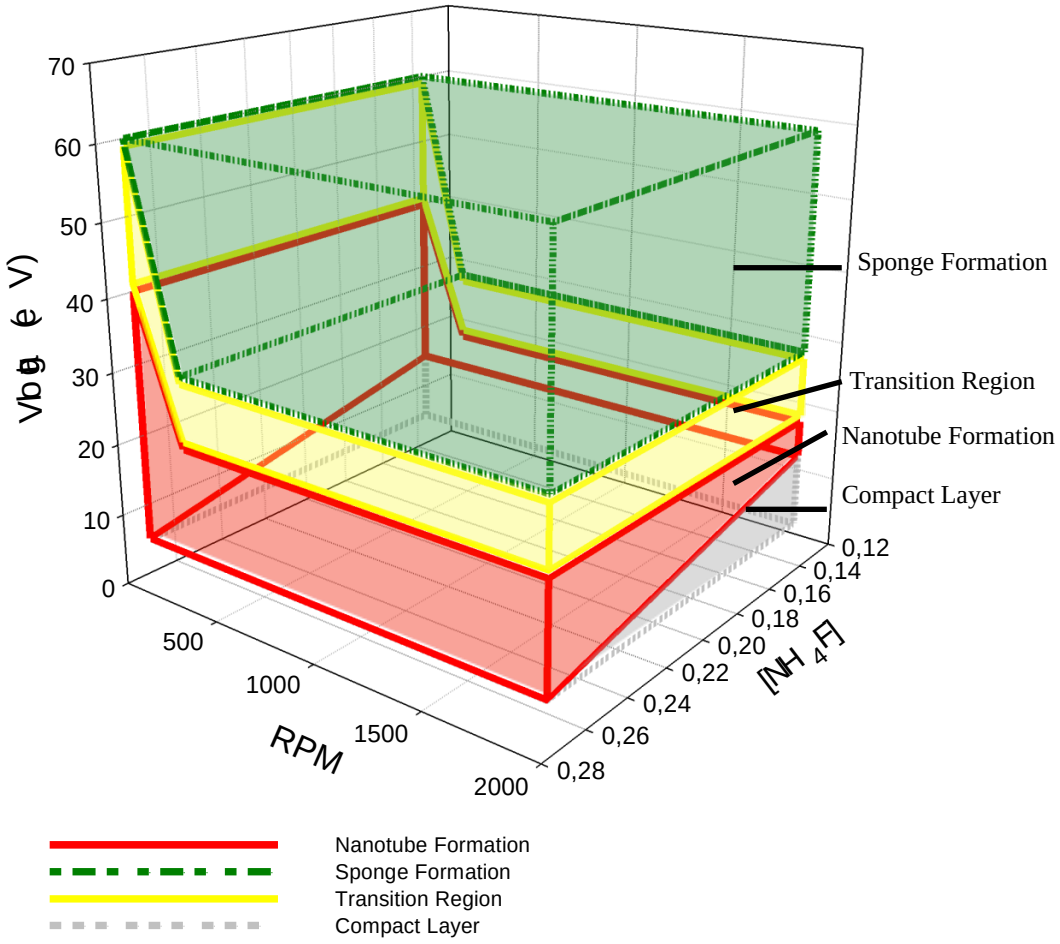
70
60
50
40
30
20
10
0
500
1000
1500
2000
RPM
0,12
0,14
0,16
0,18
0,20
0,22
0,24
0,26
0,28
Sponge Formation
Transition Region
Nanotube Formation
Compact Layer
Nanotube Formation
Sponge Formation
Transition Region
Compact Layer

Figure 3.

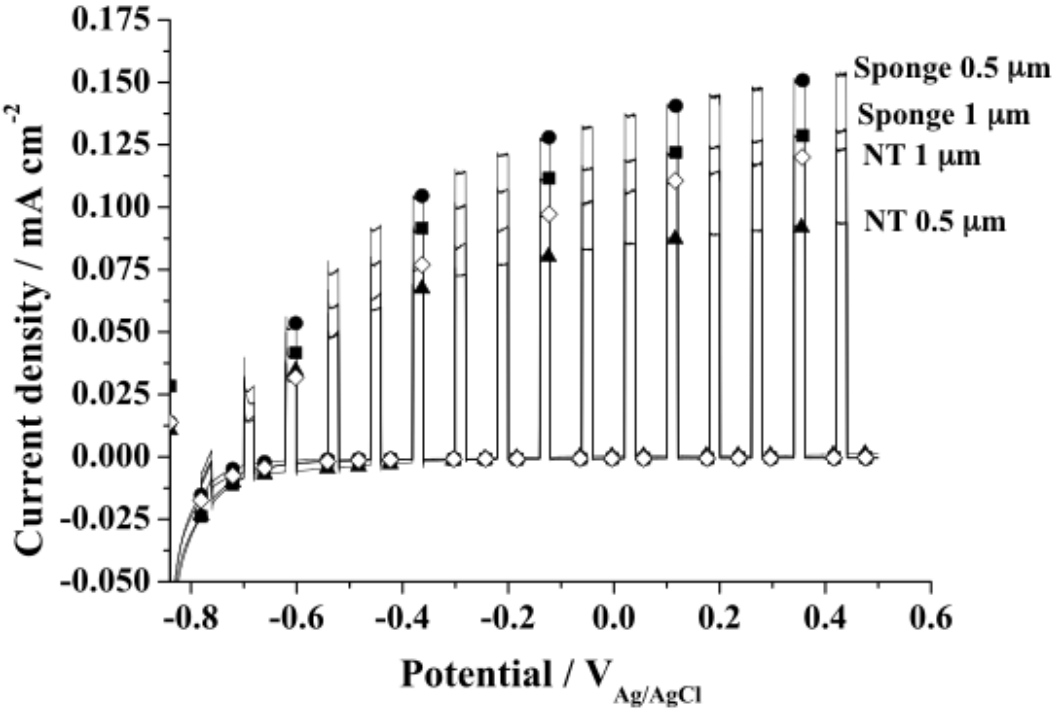
Current density / mA cm-2
0.175
0.150
0.125
0.100
0.075
0.050
0.025
0.000
-0.025
-0.050
-0.8
-0.6
-0.4
-0.2
0.0
0.2
0.4
0.6
Potential / VAg/AgCl
Sponge 0.5 μm
Sponge 1 μm
NT 1 μm
NT 0.5 μm